

## Synthesis of New Serotonin 5-HT<sub>7</sub> Receptor Ligands. Determinants of 5-HT<sub>7</sub>/5-HT<sub>1A</sub> Receptor Selectivity

Rocío A. Medina,<sup>†,‡</sup> Jessica Sallander,<sup>‡,§</sup> Bellinda Benhamú,<sup>†</sup> Esther Porras,<sup>†,||</sup> Mercedes Campillo,<sup>§</sup> Leonardo Pardo,<sup>\*,§</sup> and María L. López-Rodríguez<sup>\*,†</sup>

Departamento de Química Orgánica I, Facultad de Ciencias Químicas, Universidad Complutense de Madrid, E-28040 Madrid, Spain, and Laboratori de Medicina Computacional, Unitat de Bioestadística, Facultat de Medicina, Universitat Autònoma de Barcelona, E-08193 Bellaterra, Barcelona, Spain

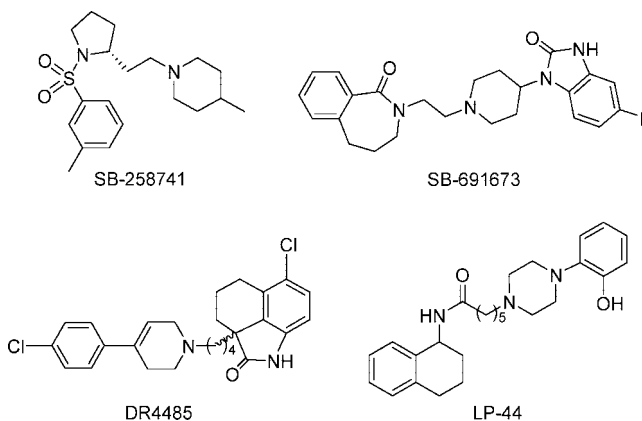
Received November 18, 2008

We report the synthesis of a new set of compounds of general structure **I** (1–20) with structural modifications in the pharmacophoric elements of the previously reported lead UCM-5600. The new derivatives have been evaluated for binding affinity at 5-HT<sub>7</sub> and 5-HT<sub>1A</sub> receptors. The influence of the different structural features in terms of 5-HT<sub>7</sub>/5-HT<sub>1A</sub> receptor affinity and selectivity was analyzed by computational simulations of the complexes between compounds **I** and  $\beta_2$ -based 3-D models of these receptors. Compound **18** (HYD<sub>1</sub> = 1,3-dihydro-2H-indol-2-one; spacer = -(CH<sub>2</sub>)<sub>4</sub>-; HYD<sub>2</sub> + HYD<sub>3</sub> = 3,4-dihydroisoquinolin-2(1H)-yl) exhibits high 5-HT<sub>7</sub>R affinity ( $K_i$  = 7 nM) and selectivity over the 5-HT<sub>1A</sub>R (31-fold), and has been characterized as a partial agonist of the human 5-HT<sub>7</sub>R.

### Introduction

Serotonin (5-hydroxytryptamine, 5-HT) is an important neurotransmitter that interacts with 14 serotonergic receptor subtypes, classified into seven families (5-HT<sub>1–7</sub>),<sup>1</sup> to elicit numerous physiological processes.<sup>2</sup> Many of these receptors (e.g., 5-HT<sub>1A</sub>, 5-HT<sub>1D</sub>, 5-HT<sub>3</sub>, 5-HT<sub>4</sub>) are tractable targets for drug discovery, with several compounds in advanced clinical development or marketed.<sup>3–5</sup> The more recently discovered 5-HT<sub>7</sub> receptor (5-HT<sub>7</sub>R),<sup>6,7</sup> first cloned in 1993,<sup>8,9</sup> has been identified in several species, including human, and is positively coupled to adenylyl cyclase via Gs proteins.<sup>10</sup> The 5-HT<sub>7</sub>R displays a low degree of homology (40%) with other serotonin G protein-coupled receptors (GPCRs). Recent distribution studies in brain have revealed a high abundance of the 5-HT<sub>7</sub>R protein in hippocampus, thalamus, hypothalamus and cerebral cortex.<sup>11</sup> In the hypothalamus, it is mainly expressed in the suprachiasmatic nucleus, which functions as the circadian clock. It is thus a potential target for sleep disturbances<sup>12</sup> such as jet lag, and for related psychiatric disorders such as mental fatigue or depression.<sup>13</sup> The presence in the hypothalamus also correlates with its involvement in thermoregulation and endocrine function.<sup>6</sup> In addition, the significant density of the 5-HT<sub>7</sub>R in the hippocampus accounts for its role in learning and memory.<sup>14</sup> The 5-HT<sub>7</sub>R subtype has also been found in smooth muscle cells and in blood vessels of the skull and other peripheral tissues,<sup>15,16</sup> so it is suggested as a putative target for migraine<sup>17</sup> and irritable bowel syndrome<sup>18</sup> treatments. All together, many important functional roles for the 5-HT<sub>7</sub>R have been reported

Chart 1. Structures of 5-HT<sub>7</sub>R Agents



in various pathophysiological processes. Therefore, this receptor has become an attractive target for drug discovery and in the past years intense efforts have led to the identification of different structural classes of 5-HT<sub>7</sub>R agents, mainly by high throughput screening of pharmaceutical companies (Chart 1).<sup>19–22</sup> Some of them have been the subject of extensive preclinical research. Nevertheless, to date there have not been many 5-HT<sub>7</sub>R ligands in clinical development programs, and current and future research should determine whether a ligand of this receptor is suitable as a therapeutic agent.

In the course of a program aimed at the discovery of new potent and selective serotonin 5-HT<sub>7</sub>R ligands, we postulated a ligand-based pharmacophore model for 5-HT<sub>7</sub>R antagonism.<sup>23,24</sup> The model consists of five features: a positive ionizable atom (PI), a H-bonding acceptor group (HBA), and three hydrophobic regions (HYD<sub>1</sub>–HYD<sub>3</sub>) (Figure 1). Other pharmacophore models of 5-HT<sub>7</sub>R agonism<sup>25</sup> and antagonism/inverse agonism<sup>26,27</sup> were reported. These models of antagonism have added to our previous proposal either a fourth hydrophobic region (HYD<sub>4</sub>)<sup>26</sup> or a second H-bonding acceptor group (HBA<sub>2</sub>).<sup>27</sup> Our pharmacophore model was validated through the design and synthesis of a series of naphtholactam and naphthosultam derivatives that led us to confirm the essential structural requirements for ligand

\* To whom correspondence should be addressed. For M.L.L.-R.: phone, 34-91-3944239; fax, 34-91-3944103; e-mail, mluzlr@quim.ucm.es. For L.P.: phone, 34-93-5812797; fax, 34-93-5812344; e-mail, Leonardo.Pardo@uab.es.

<sup>†</sup> Universidad Complutense de Madrid.

<sup>‡</sup> Both authors contributed equally.

<sup>§</sup> Universitat Autònoma de Barcelona.

<sup>||</sup> Present address: GlaxoSmithKline, Severo Ochoa 2, E-28760 Tres Cantos, Madrid, Spain.

<sup>a</sup> Abbreviations: GPCR, G protein-coupled receptor; 5-HT<sub>7</sub>R, 5-HT<sub>7</sub> receptor; 5-HT<sub>1A</sub>R, 5-HT<sub>1A</sub> receptor; PI, positive ionizable atom; HBA, H-bonding acceptor group; HYD, hydrophobic; TM, transmembrane helix; EL, extracellular loop; IL, intracellular loop.

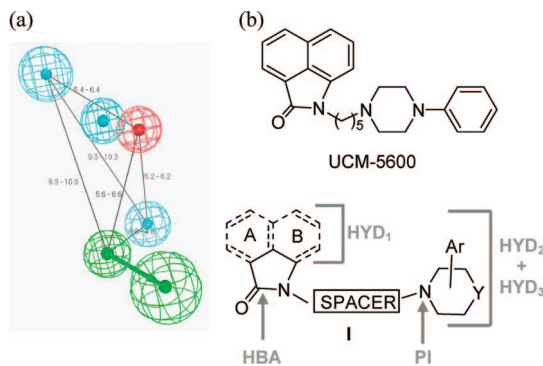


**Figure 1.** (a) Pharmacophore model proposed for 5-HT<sub>7</sub>R antagonism. (b) Lead compound UCM-5600 and compounds of general structure **I**.

recognition.<sup>24</sup> Analogue UCM-5600 ( $K_i = 89$  nM) was identified as a lead for the search of new 5-HT<sub>7</sub>R ligands. Here, we have studied a new set of compounds with structural modifications at the different pharmacophoric elements present in UCM-5600 (Figure 1). We report the synthesis of new compounds of general structure **I** and their binding affinities at 5-HT<sub>7</sub> and 5-HT<sub>1A</sub> receptors. Computational simulations of the complexes between compounds **I** and  $\beta_2$ -based 3-D models of both 5-HT receptors have permitted us to study the influence of the different structural features in terms of 5-HT<sub>7</sub>R affinity and selectivity over the 5-HT<sub>1A</sub>R. This study has provided valuable information about the molecular details of the ligand–receptor interaction in this family of compounds and has allowed us to propose a hypothesis for 5-HT<sub>7</sub>/5-HT<sub>1A</sub> receptor selectivity. This selectivity has been achieved in ligand **18** (HYD<sub>1</sub> = 1,3-dihydro-2H-indol-2-one; spacer =  $-(CH_2)_4-$ ; HYD<sub>2</sub> + HYD<sub>3</sub> = 3,4-dihydroisoquinolin-2(1H)-yl), which was pharmacologically characterized as a partial agonist of the h5-HT<sub>7</sub>R.

## Results and Discussion

**Synthesis.** Target compounds of general structure **I** (Table 1) were obtained following the synthetic routes described in Scheme 1. In general, appropriate commercially available or previously synthesized arylpiperazine or arylpiperidine was alkylated with halides **21–29** using triethylamine and acetonitrile solvent to afford final compounds **1–18** (see Experimental Section for details). Compound **10** (Ar = 4-(benzimidazol-4-yl)) was obtained by subsequent treatment with THF, acetic acid and water that was required for selective removal of the trityl protecting group in the benzimidazole ring. Bromoalkyl derivatives **21**, **22** were prepared by reduction of the corresponding 1-( $\omega$ -bromoalkyl)phthalimide with tin in hydrobromic and acetic acids, as previously reported<sup>28</sup> (Scheme 1). Intermediates **23–29** were obtained by reaction of 1,3-dihydro-2H-indol-2-one with the appropriate dihalide in the presence of K<sub>2</sub>CO<sub>3</sub> (**23–27**) or Cs<sub>2</sub>CO<sub>3</sub> (**28**, **29**) in acetonitrile solution (Scheme 1). 1-(Naphth-1-yl)piperazine (**32**) and 1-(1-tritylbenzimidazol-4-yl)piperazine (**33**) were synthesized via Pd(0)-catalyzed coupling of the corresponding aromatic halide with piperazine, following previously described procedures.<sup>29,30</sup> In the case of final compounds **19**, **20** the alkylation reaction was performed between readily available 1,3-dihydro-2H-indol-2-one and corresponding 2-( $\omega$ -haloalkyl)-1,2,3,4-tetrahydroisoquinoline **30**, **31** (Scheme 1), which were prepared by treatment of commercial 1,2,3,4-tetrahydroisoquinoline with 1,3-dibromopropane or with 2-chloroethanol followed by thionyl chloride,<sup>31</sup> respectively.

**Binding Affinities and Structure–Affinity Relationships.** New synthesized compounds **I** (**1–20**) were assessed for *in vitro* affinity at human serotonergic 5-HT<sub>7</sub> and 5-HT<sub>1A</sub> receptors

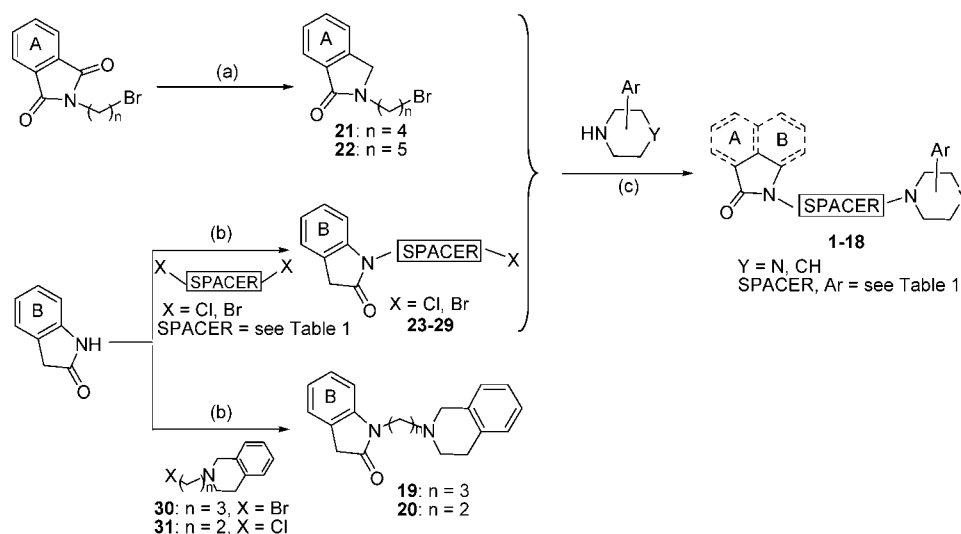
**Table 1.** Binding Affinity of Synthesized Compounds **I** (**1–20**) at 5-HT<sub>7</sub> and 5-HT<sub>1A</sub> Receptors

compd	ring	spacer	Y	Ar	$K_i \pm$ SEM (nM) <sup>a</sup>	
					5-HT <sub>7</sub>	5-HT <sub>1A</sub>
<b>1</b>	A	$-(CH_2)_4-$	N	4-phenyl	>1000	360 ± 9
<b>2</b>	A	$-(CH_2)_4-$	N	4-(2-methoxyphenyl)	158 ± 18	>1000
<b>3</b>	A	$-(CH_2)_5-$	N	4-phenyl	203 ± 24	>1000
<b>4</b>	B	$-(CH_2)_4-$	N	4-phenyl	74 ± 9	124 ± 12
<b>5</b>	B	$-(CH_2)_4-$	N	4-(2-methoxyphenyl)	32 ± 4	>1000
<b>6</b>	B	$-(CH_2)_4-$	N	4-(naphth-1-yl)	47 ± 6	22 ± 2
<b>7</b>	B	$-(CH_2)_5-$	N	4-phenyl	63 ± 8	>1000
<b>8</b>	B	$-(CH_2)_5-$	N	4-(2-methoxyphenyl)	63 ± 7	>1000
<b>9</b>	B	$-(CH_2)_5-$	N	4-(naphth-1-yl)	69 ± 2	16 ± 1
<b>10</b>	B	$-(CH_2)_5-$	N	4-(benzimidazol-4-yl)	68 ± 8	18.1 ± 0.4
<b>11</b>	B	$-(CH_2)_6-$	N	4-(naphth-1-yl)	250 ± 19	11.5 ± 0.3
<b>12</b>	B	$-(CH_2)_6-$	N	4-(naphth-1-yl)	69 ± 7	39 ± 4
<b>13</b>	B	$-(CH_2)_7-$	N	4-(naphth-1-yl)	>1000	26 ± 2
<b>14</b>	B	$-(CH_2)_8-$	N	4-(naphth-1-yl)	>1000	>1000
<b>15</b>	B	$-(CH_2)_9-$	N	4-(naphth-1-yl)	>1000	181 ± 7
<b>16</b>	B	$-(CH_2)_4-$	CH	4-phenyl	160 ± 15	>1000
<b>17</b>	B	$-(CH_2)_4-$	CH <sub>2</sub>	3-phenyl	193 ± 13	>1000
<b>18</b>	B	$-(CH_2)_4-$	3,4-dihydroisoquinolin-2(1H)-yl		7 ± 2	219 ± 11
<b>19</b>	B	$-(CH_2)_5-$	3,4-dihydroisoquinolin-2(1H)-yl		105 ± 12	>1000
<b>20</b>	B	$-(CH_2)_5-$	3,4-dihydroisoquinolin-2(1H)-yl		350 ± 25	>1000
UCM-5600	AB	$-(CH_2)_4-$	N	4-phenyl	89 ± 5 <sup>b</sup>	92% <sup>c</sup>

<sup>a</sup> Values are the mean of two to four experiments performed in triplicate.

<sup>b</sup> Value from ref 24. <sup>c</sup> Displacement of radioligand at 1  $\mu$ M concentration.

by radioligand binding assays, using [<sup>3</sup>H]LSD in transfected CHO-K1 cells and [<sup>3</sup>H]-8-OH-DPAT in transfected HEK-293 cells, respectively (see Experimental Section for details). All compounds were assayed as hydrochloride salts. The competitive inhibition assays were first performed at a fixed dose of 10<sup>-6</sup> M, and the complete dose–response curve, at six different concentrations of the ligand, was determined for those compounds that presented a displacement of the radioligand over 55%. The inhibition constant  $K_i$  was calculated from the IC<sub>50</sub> value using the Cheng–Prusoff equation,<sup>32</sup> and the values in Table 1 are the mean of two to four experiments. The following structure–affinity relationships can be drawn from the binding affinity data presented in Table 1. (a) The isoindolin-1-one moiety (ring A) is a less favorable HYD<sub>1</sub> region than the 1,3-dihydro-2H-indol-2-one system (ring B) for 5-HT<sub>7</sub>R affinity, since compounds **1–3** ( $K_i(\mathbf{1}) > 1000$  nM,  $K_i(\mathbf{2}) = 158$  nM,  $K_i(\mathbf{3}) = 203$  nM) display much lower affinity than related derivatives **4**, **5**, and **7** ( $K_i(\mathbf{4}) = 74$  nM,  $K_i(\mathbf{5}) = 32$  nM,  $K_i(\mathbf{7}) = 63$  nM), respectively. (b) In agreement with the optimum length (5.2–6.2 Å) between HYD<sub>1</sub> and the basic center PI proposed in our pharmacophore model (see Figure 1), a spacer containing at least four methylene units is necessary for high 5-HT<sub>7</sub>R affinity. Notably, binding affinity is decreased when the length is progressively shortened from four to three and two methylenes in compounds **19** and **20** ( $K_i(\mathbf{19}) = 105$  nM,  $K_i(\mathbf{20}) = 350$  nM *vs*  $K_i(\mathbf{18}) = 7$  nM). However, these ligands become selective over the 5-HT<sub>1A</sub>R ( $K_i > 1000$  nM). It is also observed that a

Scheme 1<sup>a</sup>

<sup>a</sup> Reagents and conditions: (a) Sn, HBr, acetic acid, reflux, 6 h; (b)  $K_2CO_3$  or  $Cs_2CO_3$ , acetonitrile, reflux, 3–5 h; (c) (1)  $Et_3N$ , acetonitrile, 60 °C, 24 h; (2) **10**: THF/acetic acid/ $H_2O$ , reflux, 3 h.

saturated alkyl chain is preferred for binding the 5-HT<sub>7</sub>R. Indeed, unsaturated analogues **11**, **13–15** are poorly active or inactive ( $K_i(\mathbf{11}) = 250$  nM,  $K_i(\mathbf{13–15}) >1000$  nM) in contrast with related saturated derivatives **6** and **9** ( $K_i(\mathbf{6}) = 47$  nM,  $K_i(\mathbf{9}) = 69$  nM). Only unsaturated compound **12**, with a *trans* double bond in the spacer, conserves 5-HT<sub>7</sub>R affinity ( $K_i(\mathbf{12}) = 69$  nM). (c) HYD<sub>2</sub> and HYD<sub>3</sub> pharmacophoric regions seem to play an important role in 5-HT<sub>7</sub>/5-HT<sub>1A</sub> receptor selectivity. Thus, compounds **5**, **7**, **8**, and **18**, containing a monocyclic system as HYD<sub>3</sub>, exhibit affinity for the 5-HT<sub>7</sub>R and are inactive or poorly active at the 5-HT<sub>1A</sub>R; whereas compounds **6**, **9**, **10**, and **12**, containing bicyclic moieties, exhibit affinity for both receptors.

#### Computational Models of 5-HT<sub>7</sub> and 5-HT<sub>1A</sub> Receptors in Complex with Ligands I.

In an attempt to get a better understanding of the ligand–receptor interactions involved in 5-HT<sub>7</sub>/5-HT<sub>1A</sub> receptor affinity and selectivity, we have performed computational simulations of the complexes between compounds of general structure **I** and both receptors (see Experimental Section for details). The amino acid residues of aminergic GPCRs involved in ligand binding have been identified by site-directed mutagenesis within transmembrane helices (TMs) 3, 5, 6, and 7; and extracellular loop (EL) 2.<sup>33</sup> This has been confirmed by the recent crystal structures of the  $\beta_1$ - and  $\beta_2$ -adrenergic receptors bound to the antagonist cyanopindolol<sup>34</sup> and the partial inverse agonist carazolol,<sup>35,36</sup> respectively. In addition, we have recently proposed that the aromatic moiety of antagonists of the GPCR family occupy a small cavity between TMs 5 and 6, and act by blocking the proposed conformational transition of W6.48 of the highly conserved CWxPF motif in TM 6 and the subsequent steps in the activation process.<sup>37</sup> Thus, in the complex of compound **6** with the 5-HT<sub>7</sub>R (Figure 2a) the aromatic ring B (HYD<sub>1</sub> pharmacophoric feature) enters this cavity to interact with the aromatic side chains of F5.47 and F6.52; the carbonyl group (HBA) hydrogen bonds S6.55; the protonated amine (PI) forms an ionic interaction with D3.32; and the naphthalene ring (HYD<sub>2</sub> + HYD<sub>3</sub>) expands toward TMs 2 and 3 to interact with F3.28. Figure 2b shows the binding of compound **6** to the 5-HT<sub>1A</sub>R. Despite compound **6** shows similar binding affinity for 5-HT<sub>1A</sub>R and 5-HT<sub>7</sub>R receptors, the proposed binding mode is different. The carbonyl group (HBA) of compound **6** hydrogen bonds S5.42 of the 5-HT<sub>1A</sub>R rather than S6.55, as in the 5-HT<sub>7</sub>R.

Figure 3 shows the sequence alignment of TMs 2, 3, 5–7 of 5-HT<sub>7</sub> and 5-HT<sub>1A</sub> receptors. The absence of S6.55 in the 5-HT<sub>1A</sub>R, which contains Ala at this position, causes compound **6** to hydrogen bond S5.42. Notably, the environment of TM 5 is identical in both receptors, containing S5.42, T5.43, and A5.46; and the bulky V3.33 in TM 3, which points toward TM 5, defining the binding site crevice. Thus, it is important to remark that compound **6** could also bind the 5-HT<sub>7</sub>R in a similar manner to the 5-HT<sub>1A</sub>R, i.e. via S5.42. Compounds of general formula **I** containing structurally different spacers were designed to experimentally probe the proposed different binding modes to 5-HT<sub>1A</sub>R and 5-HT<sub>7</sub>R receptors. First, we designed unsaturated derivatives **11**, with a *cis* double bond in the spacer (Figure 2c, pink compound), and **12**, with a *trans* double bond (Figure 2c, blue compound), which superimpose with the different conformations of compound **6** in the binding to the 5-HT<sub>1A</sub>R (via S5.42, Figure 2b) and in the binding to the 5-HT<sub>7</sub>R (via S6.55, Figure 2a), respectively. Notably, constrained derivative **11** exhibits similar binding affinity for the 5-HT<sub>1A</sub>R ( $K_i(\mathbf{6}) = 22$  nM *vs*  $K_i(\mathbf{11}) = 11.5$  nM) and decreases the binding affinity for the 5-HT<sub>7</sub>R ( $K_i(\mathbf{6}) = 47$  nM *vs*  $K_i(\mathbf{11}) = 250$  nM), supporting the proposed binding modes. *Trans* analogue **12** probably retains enough flexibility to bind both the 5-HT<sub>1A</sub>R ( $K_i(\mathbf{6}) = 22$  nM *vs*  $K_i(\mathbf{12}) = 39$  nM) and the 5-HT<sub>7</sub>R ( $K_i(\mathbf{6}) = 47$  nM *vs*  $K_i(\mathbf{12}) = 69$  nM). This influence of the *cis/trans* conformation of the spacer in the 5-HT<sub>7</sub>/5-HT<sub>1A</sub> receptor selectivity is in agreement with previous results.<sup>38</sup> The triple bond in unsaturated compound **13** directs the carbonyl group (HBA feature) to S5.42, maintaining the affinity for the 5-HT<sub>1A</sub>R ( $K_i = 26$  nM). However, **13** becomes inactive at the 5-HT<sub>7</sub>R ( $K_i >1000$  nM), probably due to the fact that the rigidity of the triple bond does not permit the naphthalene ring to accommodate into the small cavity between TMs 2 and 7 and ELs 1 and 2 in the 5-HT<sub>7</sub>R, but it does into the larger 5-HT<sub>1A</sub>R cavity (see below). Second, we designed derivatives **19** and **20** in which the number of methylene units in the spacer was decreased to three and two, respectively, to impede binding to the more distant S5.42 and force binding to the closer S6.55 (see Figure 2h). In agreement, compounds **19** and **20** keep moderate 5-HT<sub>7</sub>R binding affinity ( $K_i(\mathbf{18}) = 7$  nM *vs*  $K_i(\mathbf{19}) = 105$  nM,  $K_i(\mathbf{20}) = 350$  nM), and are unable to bind the 5-HT<sub>1A</sub>R ( $K_i(\mathbf{18}) = 219$  nM *vs*  $K_i(\mathbf{19}) >1000$  nM,  $K_i(\mathbf{20}) >1000$  nM). In compound **9**, the spacer of

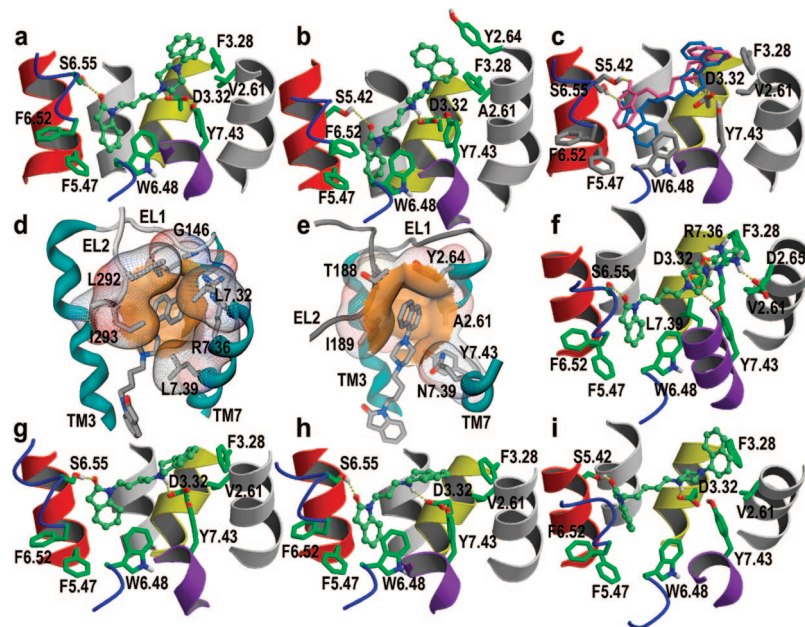


**Figure 2.** (a, b) Computational models of the complexes between compound **6** and (a) the 5-HT<sub>7</sub> and (b) 5-HT<sub>1A</sub> receptors, constructed from the crystal structure of the  $\beta_2$ -adrenergic receptor. The protonated amine of compound **6** is predicted to form an ionic interaction with D3.32; ring B, located in a small hydrophobic cavity between TMs 5 and 6, performs aromatic–aromatic interactions with the side chains of F5.47 and F6.52; the carbonyl group hydrogen bonds to S6.55 in the 5-HT<sub>7</sub>R, and to S5.42 in the 5-HT<sub>1A</sub>R; and the naphthalene aromatic ring interacts with F3.28 in the 5-HT<sub>7</sub>R, and with both F3.28 and Y2.64 in the 5-HT<sub>1A</sub>R. (c) Molecular models of the complexes between unsaturated compounds **11**, with a *cis* double bond in the spacer (pink); and **12**, with a *trans* double bond (blue), and the 5-HT<sub>7</sub>R. (d, e) The binding cavity between TMs 2, 3 and 7 and ELs 1 and 2 is larger for the (e) 5-HT<sub>1A</sub>R than for the (d) 5-HT<sub>7</sub>R. (f, g) Computational model of the complexes between compounds **5** (f), with a methoxyphenyl moiety; and **18** (g), with a benzofused aromatic ring, and the 5-HT<sub>7</sub>R. (h, i) Molecular models of the complexes between compounds **19** (h), with three methylene units in the spacer; and **9** (i), with five methylene units, and the 5-HT<sub>7</sub>R. The C $\alpha$  traces of TMs 2 (gray), 3 (yellow), 4 (gray), 5 (red), 6 (blue), and 7 (purple) are shown.

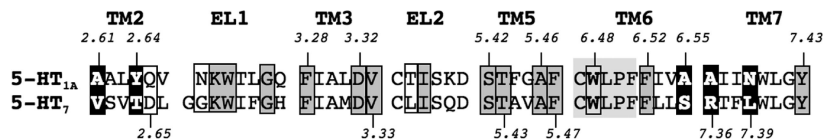


**Figure 3.** Sequence alignment of TMs 2, 3, 5–7 and ELs 1 and 2 of 5-HT<sub>1A</sub> and 5-HT<sub>7</sub> receptors. Residues referenced in the manuscript are boxed. “Hot-spots”, residues with an important contribution to the selective binding of ligands to their receptors, are in black; identical residues in dark gray; and dissimilar residues in white. The highly conserved CWXPF motif in TM6 is shown in light gray.

five methylene units favors binding to the more distant S5.42 (Figure 2i); accordingly, **9** maintains binding affinity for both 5-HT<sub>7</sub> and 5-HT<sub>1A</sub> receptors. Thus, these data point to S6.55 as a “hot spot”, i.e. residues with an important contribution to the selective binding of ligands to their receptors.

Figure 2f shows the model of the complex between the 5-HT<sub>7</sub>R and compound **5** that contains an *o*-methoxyphenyl moiety in the HYD<sub>3</sub> region instead of the naphthalene ring of compound **6** (Figure 2a). The polar methoxy group of compound **5** hydrogen bonds R7.36 of the 5-HT<sub>7</sub>R, which is also forming an ionic interaction with D2.65 (Figure 2f). The absence of both residues in the 5-HT<sub>1A</sub>R (Figure 3) explains the observed selectivity of compound **5** (5-HT<sub>7</sub>:  $K_i = 32$  nM, 5-HT<sub>1A</sub>:  $K_i > 1000$  nM), in contrast with compound **6** that exhibits high affinity for both receptors (5-HT<sub>7</sub>:  $K_i = 47$  nM, 5-HT<sub>1A</sub>:  $K_i = 22$  nM). This data points to R7.36 as another important element for 5-HT<sub>7</sub>/5-HT<sub>1A</sub> receptor selectivity, as has been previously proposed.<sup>27</sup>

Other “hot spots” in the selectivity of 5-HT<sub>7</sub>R ligands over the 5-HT<sub>1A</sub>R are located within TMs 2 and 7 and ELs 1 and 2. The 5-HT<sub>7</sub>R contains, in front of D3.32, the bulky V2.61 and L7.39 residues that are Ala and Asn, respectively, in the 5-HT<sub>1A</sub>R (Figure 3) and, thus, defining the size of the binding site between TMs 2 and 7 (Figures 2d and 2e). EL1 is one amino

acid longer in the 5-HT<sub>7</sub>R than in the 5-HT<sub>1A</sub>R, also restricting the size of the binding site; and the 5-HT<sub>7</sub>R possesses the bulky L232 instead of T188 in the 5-HT<sub>1A</sub>R (Figure 3). Moreover, near this recognition cavity D2.65 in the 5-HT<sub>7</sub>R is interacting with R7.36, absent in the 5-HT<sub>1A</sub>R, which provides additional rigidity to this hydrophobic pocket in the 5-HT<sub>7</sub>R. Therefore, the cavity between TMs 2, 3 and 7 to accommodate the ligand is smaller in the 5-HT<sub>7</sub>R than in the 5-HT<sub>1A</sub>R (Figures 2d and 2e). Accordingly, the smaller the hydrophobic moiety of the ligand placed into this small cavity, the better the binding affinity for the 5-HT<sub>7</sub>R should be. In this way compound **18** ( $K_i = 7$  nM), with a benzofused aromatic system in the HYD<sub>2</sub> + HYD<sub>3</sub> region, possesses higher binding affinity than compounds with larger HYD<sub>2</sub> + HYD<sub>3</sub> moieties [e.g., **4** ( $K_i = 74$  nM), **6** ( $K_i = 47$  nM), and **16** ( $K_i = 160$  nM)]. Figure 2g shows compound **18** into the 5-HT<sub>7</sub>R. Indeed, the tetrahydroisoquinoline ring of **18** is optimally placed into this cavity, without clashing with V2.61, and interacting with F3.28. The 5-HT<sub>1A</sub>R, in addition of possessing a larger cavity, incorporates Y2.64 toward this binding cavity that is Thr in the 5-HT<sub>7</sub>R (Figure 3). Thus, the presence of both Y2.64 and F3.28 in the 5-HT<sub>1A</sub>R allows the large naphthalene ring of compound **6** ( $K_i = 22$  nM) to interact with these aromatic residues (Figure 2e) more properly than the tetrahydroisoquinoline ring of **18** ( $K_i = 219$  nM). Thus,

compounds **5**, **7**, **8**, **16–20** with a monocyclic system as HYD<sub>3</sub> moiety are inactive or poorly active at the 5-HT<sub>1A</sub>R whereas those with a bicyclic moiety exhibit affinity for both receptors (**6**, **9**, **10**, and **12**).

**Functional Activity of Ligand 18 on the 5-HT<sub>7</sub>R.** The agonist and antagonist effects of selective ligand **18** were assessed by determining the adenylate cyclase activity in CHO cells expressing the human 5-HT<sub>7</sub>R.<sup>39</sup> Cells were treated with the ligand for 45 min at 37 °C, in the absence (agonist effect) or the presence (antagonist effect) of serotonin (100 nM), and the cAMP content was then measured by homogeneous time-resolved fluorescence (HTRF) (see Experimental Section for details). Adenylate cyclase activity is expressed as the percentage of the maximal effect obtained with serotonin. Compound **18** produced an increase of cAMP levels in a dose-dependent manner. The concentration that produced the half-maximal effect (EC<sub>50</sub>) was 0.31 ± 0.04 μM, and the maximal activation effect was 40 ± 1%. After pretreatment with serotonin, ligand **18** induced a decrease of cAMP concentration in a dose-dependent manner. The IC<sub>50</sub> value was above the highest tested concentration of 10 μM, and the maximal inhibitory effect was 43 ± 4%. Serotonin (EC<sub>50</sub> = 15 nM) and mesulergine (IC<sub>50</sub> = 120 nM) were assayed as agonist and antagonist reference compounds, respectively. These results indicate that compound **18** behaves as a partial agonist at the h5-HT<sub>7</sub>R.

The molecular mechanism underlying GPCR agonism is a key subject in medicinal chemistry. To date, there is not a clear idea as to the rearrangements occurring at the extracellular domain of serotonin receptors upon 5-HT stimulation. However, it has been proposed for other GPCRs that TM 6 performs an inward movement of the extracellular part toward TM 3 (the global toggle switch of Schwartz et al.) that is stabilized by the interaction with agonists.<sup>40</sup> The hydrogen bond interaction between compound **18** and S6.55 (Figure 2g) probably induces this proposed active conformation of TM 6. In addition, agonist binding also triggers the rotamer toggle switch of W6.48 (conserved in 71% of rhodopsin-like GPCRs) of the CWxP(F/Y) motif in TM 6, that undergoes a conformational transition from the inactive *gauche*<sup>+</sup> (pointing toward TM 7) to the active *trans* (toward TM 5) conformation,<sup>37,41</sup> which can be directly stabilized by agonist binding.<sup>42</sup> Notably, the aromatic ring B (HYD<sub>1</sub> pharmacophoric feature) of compound **18** (Figure 2g) blocks this conformational transition of W6.48 by occupying the small cavity between TMs 5 and 6 that accommodate the *trans* conformation of the W6.48 side chain in the active state of the receptor. This dual function of compound **18** might explain its pharmacological profile of partial agonist.

## Conclusions

Herein we report the synthesis of a new set of compounds of general structure **I** with structural modifications in the pharmacophoric elements of the previously reported lead UCM-5600<sup>24</sup> (Figure 1), and their binding affinities at 5-HT<sub>7</sub> and 5-HT<sub>1A</sub> receptors. Using computational models of the complexes between new ligands **I** and both receptors, we have analyzed the influence of the different structural features in 5-HT<sub>7</sub>/5-HT<sub>1A</sub> receptor affinity and selectivity. In the interaction model with the 5-HT<sub>7</sub>R, the protonated amine (PI pharmacophoric element) of the ligand forms an ionic interaction with D3.32; the aromatic ring (HYD<sub>2</sub> + HYD<sub>3</sub>) expands toward TM 7 to interact with F3.28; the carbonyl group (HBA) hydrogen bonds S6.55; and the dihydroindolone ring (HYD<sub>1</sub>) enters into a small cavity between TMs 5 and 6, to interact with the aromatic side chains of F5.47 and F6.52 (Figures 2a and 2g). This study has also

provided valuable information about the molecular determinants of 5-HT<sub>7</sub>/5-HT<sub>1A</sub> receptor selectivity. The major differences between both receptors are as follows: S6.55 is present only in the 5-HT<sub>7</sub>R whereas the 5-HT<sub>1A</sub>R contains Ala at this position; the 5-HT<sub>7</sub>R possesses the ionic D2.65•••R7.36 interaction that is absent in the 5-HT<sub>1A</sub>R; the 5-HT<sub>7</sub>R contains the bulky V2.61 and L7.39 residues that are Ala and Asn, respectively, in the 5-HT<sub>1A</sub>R; and Tyr replaces T2.64 of the 5-HT<sub>7</sub>R (Figures 2 and 3). Thus, a decrease of the distance between PI and HBA features forces the ligand to bind S6.55, increasing selectivity; polar substitutions at the HYD<sub>2</sub> + HYD<sub>3</sub> region might interact with R7.36, increasing selectivity; and an increase of the size of HYD<sub>2</sub> + HYD<sub>3</sub> region clashes with V2.61 in the 5-HT<sub>7</sub>R and favors the interaction with Y2.64 in the 5-HT<sub>1A</sub>R, decreasing selectivity.

Aimed 5-HT<sub>7</sub>/5-HT<sub>1A</sub> receptor selectivity (31-fold) has been achieved in ligand **18** (HYD<sub>1</sub> = 1,3-dihydro-2*H*-indol-2-one; spacer = -(CH<sub>2</sub>)<sub>4</sub>-; HYD<sub>2</sub> + HYD<sub>3</sub> = 3,4-dihydroisoquinolin-2(1*H*)-yl), which was pharmacologically characterized as a partial agonist. These hypotheses provide the basis for the design and development of new specific 5-HT<sub>7</sub>R ligands with predetermined pharmacological properties.

## Experimental Section

**Chemistry.** Melting points (uncorrected) were determined on a Stuart Scientific electrothermal apparatus. Infrared (IR) spectra were measured on a Bruker Tensor 27 instrument equipped with a Specac ATR accessory of 5200–650 cm<sup>-1</sup> transmission range; frequencies ( $\nu$ ) are expressed in cm<sup>-1</sup>. Nuclear magnetic resonance (NMR) spectra were recorded on a Bruker Avance 300 AM (<sup>1</sup>H, 300 MHz; <sup>13</sup>C, 75 MHz) or Bruker 200-AC spectrometer (<sup>1</sup>H, 200 MHz; <sup>13</sup>C, 50 MHz) at the UCM's NMR facilities. Chemical shifts ( $\delta$ ) are expressed in parts per million relative to internal tetramethylsilane; coupling constants (*J*) are in hertz (Hz). The following abbreviations are used to describe peak patterns when appropriate: s (singlet), d (doublet), t (triplet), qt (quintet), m (multiplet). Mass spectrometry (MS) was carried out on a Bruker LC-Esquire or a single quadrupole Agilent (1100 series) instrument in electrospray mode (ESI). Elemental analyses (C, H, N) were obtained on a LECO CHNS-932 apparatus at the UCM's analysis services and were within 0.4% of the theoretical values, confirming a purity of at least 95% for all tested compounds. Analytical thin-layer chromatography (TLC) was run on Merck silica gel plates (Kieselgel 60 F-254) with detection by UV light, iodine, ninhydrin solution, or 10% phosphomolybdic acid solution in ethanol. Flash chromatography was performed on glass column using silica gel type 60 (Merck, particle 230–400 mesh) or on a Supelco VersaFlash station using silica gel cartridges (Supelco, particle size 20–45 μM). Unless stated otherwise, starting materials, reagents and solvents were purchased as high-grade commercial products from Sigma, Aldrich, Fluka, Lancaster, Scharlab or Panreac, and were used without further purification.

The following compounds were synthesized according to described procedures: 2-(4-bromobutyl)isoindolin-1-one (**21**),<sup>28</sup> 1-(4-bromobutyl)-1,3-dihydro-2*H*-indol-2-one (**23**),<sup>43</sup> 1-(5-bromopentyl)-1,3-dihydro-2*H*-indol-2-one (**24**),<sup>43</sup> 2-(2-chloroethyl)-1,2,3,4-tetrahydroisoquinoline (**31**),<sup>31</sup> 1-(naphth-1-yl)piperazine (**32**),<sup>29</sup> 1-(1-tritylbenzimidazol-4-yl)piperazine (**33**).<sup>30</sup> Collected data for compounds **1–20** refer to free bases, and then hydrochloride salts were prepared prior to melting point determination, elemental analyses, and biological assays. Spectroscopic data of all described compounds were consistent with the proposed structures. For series **25–29** and **1–18** we include the data of compounds **25**, **28**, **2**, **3**, **6**, **10**, **16–18**.

**General Procedure for the Synthesis of Intermediate Compounds 25–29.** To a stirred solution of 1,3-dihydro-2*H*-indol-2-one (0.80 g, 6 mmol) and of the appropriate commercial dihalide (8 mmol) in anhydrous acetonitrile (90 mL), K<sub>2</sub>CO<sub>3</sub> (1.66 g, 12

mmol) or Cs<sub>2</sub>CO<sub>3</sub> (2.90 g, 9 mmol) was added. The reaction mixture was heated at reflux under an argon atmosphere for 3–5 h, then cooled to room temperature and filtered. The resulting solution was evaporated under vacuum, and the crude material was resuspended in water and extracted with dichloromethane (3 × 30 mL). The organic layers were dried (Na<sub>2</sub>SO<sub>4</sub>), filtered and evaporated under reduced pressure. The obtained residue was purified by column chromatography using the appropriate eluent, to afford pure **25–29**.

**1-[(2Z)-4-Chlorobut-2-enyl]-1,3-dihydro-2H-indol-2-one (25)**. Obtained from 1,3-dihydro-2H-indol-2-one and (2Z)-1,4-dichlorobut-2-ene, in 27% yield. Chromatography: hexane/ethyl acetate, from 8.5:1.5 to 8:2; mp 76–78 °C. IR (CHCl<sub>3</sub>): 1708, 1616, 1488, 1465 cm<sup>-1</sup>. <sup>1</sup>H NMR (CDCl<sub>3</sub>): δ 3.48 (s, 2H), 4.19 (d, *J* = 7.8, 2H), 4.39 (d, *J* = 6.7, 2H), 5.51–5.63 (m, 1H), 5.76–5.89 (m, 1H), 6.79 (d, *J* = 7.6, 1H), 6.98 (t, *J* = 7.4, 1H), 7.17–7.24 (m, 2H). <sup>13</sup>C NMR (CDCl<sub>3</sub>): δ 35.7, 36.5, 38.6, 108.5, 122.5, 124.5, 127.9, 128.4, 129.2, 144.4, 175.0. MS (ESI) 222.0 (M + H)<sup>+</sup>.

**1-[(2E)-4-Chlorobut-2-enyl]-1,3-dihydro-2H-indol-2-one (26)**. Obtained from 1,3-dihydro-2H-indol-2-one and (2E)-1,4-dichlorobut-2-ene, in 25% yield. Chromatography: hexane/ethyl acetate, 9.5:0.5; mp 72–74 °C.

**1-(4-Chlorobut-2-ynyl)-1,3-dihydro-2H-indol-2-one (27)**. Obtained from 1,3-dihydro-2H-indol-2-one and 1,4-dichlorobut-2-yne, in 25% yield. Chromatography: hexane/ethyl acetate, 8:2; mp 69–72 °C.

**1-[3-(Bromomethyl)benzyl]-1,3-dihydro-2H-indol-2-one (28)**. Obtained from 1,3-dihydro-2H-indol-2-one and 1,3-bis(bromomethyl)benzene, in 20% yield. Chromatography: hexane/ethyl acetate, 8:2; mp 111–113 °C. IR (CHCl<sub>3</sub>): 1712, 1614, 1487, 1465 cm<sup>-1</sup>. <sup>1</sup>H NMR (CDCl<sub>3</sub>): δ 3.56 (s, 2H), 4.38 (s, 2H), 4.84 (s, 2H), 6.64 (d, *J* = 7.7, 1H), 6.95 (t, *J* = 7.5, 1H), 7.09–7.27 (m, 6H). <sup>13</sup>C NMR (CDCl<sub>3</sub>): δ 33.2, 35.8, 43.6, 109.0, 122.6, 124.6, 127.5, 128.0, 128.1, 128.5, 129.4, 136.7, 138.5, 144.3, 175.2. MS (ESI) 316.0 (M + H)<sup>+</sup>.

**1-[4-(Bromomethyl)benzyl]-1,3-dihydro-2H-indol-2-one (29)**. Obtained from 1,3-dihydro-2H-indol-2-one and 1,4-bis(bromomethyl)benzene, in 20% yield. Chromatography: dichloromethane; mp 115–117 °C.

**Synthesis of 2-(3-Bromopropyl)-1,2,3,4-tetrahydroisoquinoline (30)**. To a stirred solution of 1,2,3,4-tetrahydroisoquinoline (1.87 mL, 15 mmol) in acetone (20 mL)/NaOH (3 mL), 1,3-dibromopropane (2.03 mL, 20 mmol) was added, and the reaction was stirred at room temperature for 7 h. The solvent was evaporated to dryness, and the residue was resuspended in water and extracted with dichloromethane. The organic layers were dried (Na<sub>2</sub>SO<sub>4</sub>), the solvent was evaporated under reduced pressure, and the crude material was purified by column chromatography using hexane/ethyl acetate, 9.5:0.5, to afford pure **30** in 25% yield. IR (CHCl<sub>3</sub>): 1649, 1498, 1453 cm<sup>-1</sup>. <sup>1</sup>H NMR (CDCl<sub>3</sub>): δ 2.16 (qt, *J* = 6.6, 2H), 2.66 (t, *J* = 6.9, 2H), 2.71 (t, *J* = 5.9, 2H), 2.90 (t, *J* = 5.9, 2H), 3.51 (t, *J* = 6.6, 2H), 3.63 (s, 2H), 6.93–7.62 (m, 4H). <sup>13</sup>C NMR (CDCl<sub>3</sub>): δ 29.1, 30.3, 31.9, 51.0, 56.2, 56.3, 125.6, 126.2, 126.5, 128.7, 132.4, 135.4. MS (ESI) 254.0 (M + H)<sup>+</sup>.

**General Procedure for the Synthesis of Final Compounds 1–18**. To a suspension of corresponding intermediate **21–29** (0.9 mmol) and commercially available or synthesized cyclic amine (1.5 mmol) in anhydrous acetonitrile (4 mL), triethylamine was added (0.2 mL, 1.5 mmol). The reaction mixture was heated at 60 °C under an argon atmosphere for 24 h. Upon cooling to room temperature, the solvent was evaporated under reduced pressure and the crude material was resuspended in water and extracted with dichloromethane (3 × 10 mL). The organic layers were dried (Na<sub>2</sub>SO<sub>4</sub>), filtered and evaporated, and the resulting oil was purified by column chromatography using the appropriate eluent, to provide pure **1–18**.

**2-[4-(4-Phenylpiperazin-1-yl)butyl]isoindolin-1-one (1)**. Obtained from **21** and 1-phenylpiperazine, in 62% yield. Chromatography: ethyl acetate; mp 232–234 °C (dec). Anal. (C<sub>22</sub>H<sub>27</sub>N<sub>3</sub>O·2HCl·3H<sub>2</sub>O) C, H, N.

**2-[4-[4-(2-Methoxyphenyl)piperazin-1-yl]butyl]isoindolin-1-one (2)**. Obtained from **21** and 1-(2-methoxyphenyl)piperazine, in 80% yield. Chromatography: from ethyl acetate/ethanol, 9:1 to 8:2; mp 230–232 °C (dec). IR (CHCl<sub>3</sub>): 1678, 1622, 1595, 1500, 1472, 1456 cm<sup>-1</sup>. <sup>1</sup>H NMR (CDCl<sub>3</sub>): δ 1.51–1.79 (m, 4H), 2.45 (t, *J* = 7.3, 2H), 2.63 (m, 4H), 3.07 (m, 4H), 3.65 (t, *J* = 6.8, 2H), 3.84 (s, 3H), 4.38 (s, 2H), 6.82–7.03 (m, 4H), 7.39–7.56 (m, 3H), 7.83 (dd, *J* = 7.3, 1.7, 1H). <sup>13</sup>C NMR (CDCl<sub>3</sub>): δ 24.2, 26.4, 42.2, 49.9, 50.6, 53.5, 55.4, 58.2, 111.2, 118.2, 121.0, 122.7, 122.9, 123.7, 128.0, 131.2, 133.1, 141.1, 141.4, 152.3, 168.5. MS (ESI) 380.2 (M + H)<sup>+</sup>. Anal. (C<sub>23</sub>H<sub>29</sub>N<sub>3</sub>O<sub>2</sub>·2HCl·1/2H<sub>2</sub>O) C, H, N.

**2-[5-(4-Phenylpiperazin-1-yl)pentyl]isoindolin-1-one (3)**. Obtained from **22** and 1-phenylpiperazine, in 68% yield. Chromatography: ethyl acetate; mp 188–190 °C. IR (CHCl<sub>3</sub>): 1680, 1620, 1599, 1580, 1502, 1472, 1456 cm<sup>-1</sup>. <sup>1</sup>H NMR (CDCl<sub>3</sub>): δ 1.39 (qt, *J* = 6.8, 2H), 1.52–1.78 (m, 4H), 2.38 (t, *J* = 7.3, 2H), 2.58 (t, *J* = 5.1, 4H), 3.18 (t, *J* = 5.1, 4H), 3.63 (t, *J* = 7.3, 2H), 4.38 (s, 2H), 6.80–6.94 (m, 3H), 7.25 (t, *J* = 7.1, 2H), 7.40–7.56 (m, 3H), 7.84 (dd, *J* = 8.1, 1.2, 1H). <sup>13</sup>C NMR (CDCl<sub>3</sub>): δ 24.6, 26.1, 28.2, 42.1, 48.8, 49.8, 53.0, 58.2, 116.0, 119.6, 122.5, 123.6, 127.9, 129.0, 131.1, 132.9, 141.0, 151.1, 168.4. MS (ESI) 364.2 (M + H)<sup>+</sup>. Anal. (C<sub>23</sub>H<sub>29</sub>N<sub>3</sub>O·2HCl·1/2H<sub>2</sub>O) C, H, N.

**1-[4-(4-Phenylpiperazin-1-yl)butyl]-1,3-dihydro-2H-indol-2-one (4)**. Obtained from **23** and 1-phenylpiperazine, in 79% yield. Chromatography: from ethyl acetate to ethyl acetate/ethanol, 8:2; mp 218–221 °C (dec). Anal. (C<sub>22</sub>H<sub>27</sub>N<sub>3</sub>O·HCl·4/3H<sub>2</sub>O) C, H, N.

**1-[4-[4-(2-Methoxyphenyl)piperazin-1-yl]butyl]-1,3-dihydro-2H-indol-2-one (5)**. Obtained from **23** and 1-(2-methoxyphenyl)piperazine, in 91% yield. Chromatography: ethyl acetate/ethanol, 8:2; mp 198–201 °C. Anal. (C<sub>23</sub>H<sub>29</sub>N<sub>3</sub>O<sub>2</sub>·2HCl·1/2H<sub>2</sub>O) C, H, N.

**1-[4-[4-(1-Naphthyl)piperazin-1-yl]butyl]-1,3-dihydro-2H-indol-2-one (6)**. Obtained from **23** and **32**, in 65% yield. Chromatography: ethyl acetate/hexane, 8:2; mp 226–228 °C (dec). IR (CHCl<sub>3</sub>): 1701, 1614, 1491, 1468 cm<sup>-1</sup>. <sup>1</sup>H NMR (CDCl<sub>3</sub>): δ 1.64–1.70 (m, 4H), 2.45 (t, *J* = 7.0, 2H), 2.72 (m, 4H), 3.07 (m, 4H), 3.47 (s, 2H), 3.71 (t, *J* = 7.0, 2H), 6.82 (d, *J* = 7.6, 1H), 6.93–7.03 (m, 2H), 7.17–7.33 (m, 2H), 7.38–7.42 (m, 3H), 7.48 (d, *J* = 8.3, 1H), 7.73–7.78 (m, 1H), 8.10–8.15 (m, 1H). <sup>13</sup>C NMR (CDCl<sub>3</sub>): δ 24.3, 25.4, 35.9, 39.9, 53.0, 53.8, 58.1, 108.5, 114.7, 122.2, 123.7, 124.6, 125.4, 125.8, 125.9, 127.7, 128.4, 129.3, 135.1, 144.9, 150.0, 175.5. MS (ESI) 400.1 (M + H)<sup>+</sup>. Anal. (C<sub>26</sub>H<sub>29</sub>N<sub>3</sub>O·2HCl·7/2H<sub>2</sub>O) C, H, N.

**1-[5-(4-Phenylpiperazin-1-yl)pentyl]-1,3-dihydro-2H-indol-2-one (7)**. Obtained from **24** and 1-phenylpiperazine, in 98% yield. Chromatography: ethyl acetate; mp 212–214 °C. Anal. (C<sub>23</sub>H<sub>29</sub>N<sub>3</sub>O·2HCl·1/2H<sub>2</sub>O) C, H, N.

**1-[5-[4-(2-Methoxyphenyl)piperazin-1-yl]pentyl]-1,3-dihydro-2H-indol-2-one (8)**. Obtained from **24** and 1-(2-methoxyphenyl)piperazine, in 86% yield. Chromatography: ethyl acetate; mp 195–197 °C. Anal. (C<sub>24</sub>H<sub>31</sub>N<sub>3</sub>O<sub>2</sub>·2HCl·H<sub>2</sub>O) C, H, N.

**1-[5-[4-(1-Naphthyl)piperazin-1-yl]pentyl]-1,3-dihydro-2H-indol-2-one (9)**. Obtained from **24** and **32**, in 56% yield. Chromatography: ethyl acetate/hexane, 9:1; mp 234–235 °C (dec). Anal. (C<sub>27</sub>H<sub>31</sub>N<sub>3</sub>O·HCl·H<sub>2</sub>O) C, H, N.

**1-[5-[4-(1H)-benzimidazol-4-yl]piperazin-1-yl]pentyl]-1,3-dihydro-2H-indol-2-one (10)**. 1-[5-[4-(1-trityl(1H)-benzimidazol-4-yl)piperazin-1-yl]pentyl]-1,3-dihydro-2H-indol-2-one was obtained from **24** and **33**, in 42% yield. Chromatography: ethyl acetate/ethanol, 9.5:0.5 (oil). IR (CHCl<sub>3</sub>): 1710, 1495, 1445, 1430 cm<sup>-1</sup>. <sup>1</sup>H NMR (CDCl<sub>3</sub>): δ 1.36–1.48 (m, 2H), 1.67–1.83 (m, 4H), 2.58 (t, *J* = 7.8, 2H), 3.17 (m, 4H), 3.47 (m, 4H), 3.51 (s, 2H), 3.70 (t, *J* = 7.1, 2H), 6.10 (d, *J* = 8.4, 1H), 6.54 (d, *J* = 7.8, 1H), 6.75–6.87 (m, 2H), 6.98–7.23 (m, 6H), 7.25–7.37 (m, 12H), 7.81 (s, 1H). <sup>13</sup>C NMR (CDCl<sub>3</sub>): δ 24.7, 27.1, 35.6, 39.7, 49.3, 53.0, 58.2, 75.1, 107.3, 108.1, 108.7, 121.9, 122.6, 124.2, 124.5, 127.6, 127.8, 129.8, 135.8, 136.6, 141.2, 141.5, 141.7, 142.8, 144.5, 174.8. MS (ESI) 646.2 (M + H)<sup>+</sup>.

A solution of above synthesized trityl derivative (110 mg, 0.2 mmol) in THF (1.4 mL), acetic acid (1.4 mL) and water (1.4 mL) was heated at reflux for 3 h. The mixture was cooled to room temperature, acidified with 1 M HCl until pH 1–2, and then

extracted with ethyl acetate. Anhydrous  $K_2CO_3$  was added to the aqueous layer until pH 9–10, and the basic solution was extracted with dichloromethane. The organic layers were dried ( $Na_2SO_4$ ), filtered and evaporated to provide final compound **10**, in 58% yield. IR (CHCl<sub>3</sub>): 1710, 1495, 1445, 1430 cm<sup>-1</sup>. <sup>1</sup>H NMR (CDCl<sub>3</sub>): δ 1.31–1.34 (m, 2H), 1.56–1.67 (m, 4H), 2.37 (t, *J* = 7.5, 2H), 2.66 (m, 4H), 3.46 (m, 6H), 3.64 (t, *J* = 7.2, 2H), 6.59 (t, *J* = 4.2, 1H), 6.77 (d, *J* = 7.7, 1H), 6.97 (t, *J* = 7.2, 1H), 7.08–7.30 (m, 4H), 7.92 (s, 1H). <sup>13</sup>C NMR (CDCl<sub>3</sub>): δ 24.6, 25.5, 27.1, 35.8, 39.7, 49.4, 53.0, 58.1, 107.0, 108.2, 108.3, 122.2, 123.6, 124.4, 124.5, 127.8, 135.7, 136.5, 138.7, 142.4, 144.4, 175.1. MS (ESI) 404.3 (M + H)<sup>+</sup>. Anal. (C<sub>24</sub>H<sub>29</sub>N<sub>5</sub>O·3HCl·3H<sub>2</sub>O) C, H, N.

**1-((2Z)-4-[4-(1-Naphthyl)piperazin-1-yl]but-2-enyl)-1,3-dihydro-2H-indol-2-one (11)**. Obtained from **25** and **32**, in 42% yield. Chromatography: hexane/ethyl acetate, 3:7; mp 226–228 °C (dec). Anal. (C<sub>26</sub>H<sub>27</sub>N<sub>3</sub>O·2HCl·3H<sub>2</sub>O) C, H, N.

**1-((2E)-4-[4-(1-Naphthyl)piperazin-1-yl]but-2-enyl)-1,3-dihydro-2H-indol-2-one (12)**. Obtained from **26** and **32**, in 44% yield. Chromatography: hexane/ethanol, 8:2; mp 173–175 °C (dec). Anal. (C<sub>26</sub>H<sub>27</sub>N<sub>3</sub>O·2HCl·7/2H<sub>2</sub>O) C, H, N.

**1-[4-[4-(1-Naphthyl)piperazin-1-yl]but-2-ynyl]-1,3-dihydro-2H-indol-2-one (13)**. Obtained from **27** and **32**, in 25% yield. Chromatography: hexane/ethanol, 9:1; mp 171–173 °C (dec). Anal. (C<sub>26</sub>H<sub>25</sub>N<sub>3</sub>O·2H<sub>2</sub>O·9/2HCl) C, H, N.

**1-(3-[[4-(1-Naphthyl)piperazin-1-yl]methyl]benzyl)-1,3-dihydro-2H-indol-2-one (14)**. Obtained from **28** and **32**, in 30% yield. Chromatography: hexane/ethyl acetate, 7:3; mp 209–211 °C (dec). Anal. (C<sub>30</sub>H<sub>29</sub>N<sub>3</sub>O·2HCl·7/2H<sub>2</sub>O) C, H, N.

**1-(4-[[4-(1-Naphthyl)piperazin-1-yl]methyl]benzyl)-1,3-dihydro-2H-indol-2-one (15)**. Obtained from **29** and **32**, in 25% yield. Chromatography: hexane/ethyl acetate, 7:3; mp 210–212 °C (dec). Anal. (C<sub>30</sub>H<sub>29</sub>N<sub>3</sub>O·2HCl·H<sub>2</sub>O) C, H, N.

**1-[4-(4-Phenylpiperidin-1-yl)butyl]-1,3-dihydro-2H-indol-2-one (16)**. Obtained from **23** and 4-phenylpiperidine, in 40% yield. Chromatography: hexane/ethyl acetate/ammonia, 9:1:0.1 (oil). <sup>1</sup>H NMR (CDCl<sub>3</sub>): δ 1.52–1.84 (m, 4H), 1.81–1.84 (m, 4H), 2.05 (t, *J* = 11.2, 2H), 2.42 (t, *J* = 7.1, 2H), 2.47–2.50 (m, 1H), 3.04 (d, *J* = 10.9, 2H), 3.54 (s, 2H), 3.76 (t, *J* = 6.9, 2H), 6.88 (d, *J* = 7.8, 1H), 7.04 (t, *J* = 7.5, 1H), 7.21–7.27 (m, 7H). <sup>13</sup>C NMR (CDCl<sub>3</sub>): δ 24.2, 25.3, 33.3, 35.7, 40.0, 43.6, 54.2, 58.7, 108.3, 122.0, 124.3, 126.0, 126.7, 127.7, 128.3, 143.3, 147.5, 175.2. MS (ESI) 349.0 (M + H)<sup>+</sup>. Anal. (C<sub>23</sub>H<sub>28</sub>N<sub>2</sub>O·HCl·5H<sub>2</sub>O) C, H, N.

**1-[4-(3-Phenylpiperidin-1-yl)butyl]-1,3-dihydro-2H-indol-2-one (17)**. Obtained from **23** and 3-phenylpiperidine, in 42% yield. Chromatography: hexane/ethanol/ammonia, 9:1:0.1 (oil). <sup>1</sup>H NMR (CDCl<sub>3</sub>): δ 1.36–1.90 (m, 8H), 1.96 (t, *J* = 11.2, 2H), 2.39 (t, *J* = 7.1, 2H), 2.79–2.81 (m, 1H), 2.97 (d, *J* = 10.8, 2H), 3.44 (s, 2H), 3.67 (t, *J* = 7.0, 2H), 6.78 (d, *J* = 7.6, 1H), 6.96 (t, *J* = 7.5, 1H), 7.10–7.27 (m, 7H). <sup>13</sup>C NMR (CDCl<sub>3</sub>): δ 22.7, 24.2, 31.2, 35.8, 40.1, 43.9, 53.8, 58.9, 108.4, 122.2, 124.5, 127.3, 127.8, 128.5, 144.3, 147.5, 175.2. MS (ESI) 349.0 (M + H)<sup>+</sup>. Anal. (C<sub>23</sub>H<sub>28</sub>N<sub>2</sub>O·HCl·9/2H<sub>2</sub>O) C, H, N.

**1-[4-(3,4-Dihydroisoquinolin-2(1H)-yl)butyl]-1,3-dihydro-2H-indol-2-one (18)**. Obtained from **23** and 1,2,3,4-tetrahydroisoquinoline, in 45% yield. Chromatography: hexane/ethyl acetate, 3:7 (oil). IR (CHCl<sub>3</sub>): 1701, 1614, 1558, 1489, 1468 cm<sup>-1</sup>. <sup>1</sup>H NMR (CDCl<sub>3</sub>): δ 1.69–1.78 (m, 4H), 2.56 (t, *J* = 6.0, 2H), 2.73 (t, *J* = 6.0, 2H), 2.90 (t, *J* = 6.0, 2H), 3.50 (s, 2H), 3.63 (s, 2H), 3.77 (t, *J* = 6.0, 2H), 6.87 (d, *J* = 7.8, 1H), 7.00–7.10 (m, 2H), 7.11–7.13 (m, 3H), 7.22–7.27 (m, 2H). <sup>13</sup>C NMR (CDCl<sub>3</sub>): δ 24.4, 25.3, 29.1, 35.8, 39.7, 50.9, 56.2, 57.6, 108.4, 122.1, 124.4, 124.6, 125.6, 127.8, 128.6, 134.3, 134.8, 144.6, 174.9. MS (ESI) 321.1 (M + H)<sup>+</sup>. Anal. (C<sub>21</sub>H<sub>24</sub>N<sub>2</sub>O·HCl·5/2H<sub>2</sub>O) C, H, N.

**Synthesis of 1-[3-(3,4-Dihydroisoquinolin-2(1H)-yl)propyl]-1,3-dihydro-2H-indol-2-one (19)**. A mixture of **30** (76.3 mg, 0.3 mmol), 1,3-dihydro-2H-indol-2-one (39.9 mg, 0.3 mmol), and anhydrous  $K_2CO_3$  (148 mg, 1.1 mmol) in acetone (8.9 mL) was heated at reflux for 9 h. Upon cooling the reaction to room temperature, the solid was filtered off, and the resulting solution was evaporated to dryness. The residue was purified by column chromatography eluting with hexane/ethyl acetate, from 9:1 to 8:2,

to afford pure **19** in 44% yield. IR (CHCl<sub>3</sub>): 1716, 1612, 1489, 1467 cm<sup>-1</sup>. <sup>1</sup>H NMR (CDCl<sub>3</sub>): δ 1.90 (qt, *J* = 7.0, 2H), 2.51 (t, *J* = 7.0, 2H), 2.64 (t, *J* = 6.0, 2H), 2.82 (t, *J* = 5.9, 2H), 3.42 (s, 2H), 3.54 (s, 2H), 3.75 (t, *J* = 7.0, 2H), 6.85 (d, *J* = 7.6, 1H), 7.00–7.09 (m, 2H), 7.10–7.12 (m, 3H), 7.17–7.20 (m, 2H). <sup>13</sup>C NMR (CDCl<sub>3</sub>): δ 25.1, 29.1, 35.8, 38.2, 50.9, 55.3, 56.1, 108.4, 122.1, 124.4, 124.6, 125.6, 126.1, 126.5, 127.8, 128.6, 134.3, 134.7, 144.8, 175.1. MS (ESI): 307.2 (M + 1). Anal. (C<sub>20</sub>H<sub>22</sub>N<sub>2</sub>O·HCl·3H<sub>2</sub>O) C, H, N.

**Synthesis of 1-[2-(3,4-Dihydroisoquinolin-2(1H)-yl)ethyl]-1,3-dihydro-2H-indol-2-one (20)**. To a suspension of **31** (310 mg, 1.6 mmol) and 1,3-dihydro-2H-indol-2-one (319 mg, 2.4 mmol) in anhydrous acetonitrile (7 mL), KI (26.6 mg, 0.16 mmol) was added, and the mixture was heated at 60 °C for 20 h under an argon atmosphere. The reaction was cooled to room temperature, the solvent was evaporated under reduced pressure, and the residue was then resuspended in water and extracted with dichloromethane (3 × 10 mL). The organic layers were dried ( $Na_2SO_4$ ) and evaporated, and the crude material was purified by column chromatography eluting with dichloromethane/ethyl acetate, 9:5:0.5, to give pure **20** in 55% yield. IR (CHCl<sub>3</sub>): 1711, 1614, 1490, 1467 cm<sup>-1</sup>. <sup>1</sup>H NMR (CDCl<sub>3</sub>): δ 2.71–2.83 (m, 6H), 3.46 (s, 2H), 3.70 (s, 2H), 3.92 (t, *J* = 7.2, 2H), 6.87 (d, *J* = 7.7, 1H), 7.00–7.09 (m, 2H), 7.10–7.12 (m, 3H), 7.17–7.20 (m, 2H). <sup>13</sup>C NMR (CDCl<sub>3</sub>): δ 29.1, 35.9, 38.1, 51.0, 54.7, 56.4, 108.4, 122.3, 124.6, 124.7, 125.8, 126.3, 126.6, 127.9, 128.8, 134.3, 134.8, 146.4, 174.9. MS (ESI): 293.2 (M + 1). Anal. (C<sub>19</sub>H<sub>20</sub>N<sub>2</sub>O·HCl·5/2H<sub>2</sub>O) C, H, N.

**Pharmacology. Radioligand Binding Assays.** Membranes from HEK-293 and CHO-K1 cells expressing human 5-HT<sub>7</sub> and 5-HT<sub>1A</sub> receptors, respectively, were purchased from Perkin-Elmer and conserved at –80 °C in packaging buffer for subsequent use. Specific radioligands [<sup>3</sup>H]LSD (79.2 Ci/mmol) and [<sup>3</sup>H]-8-OH-DPAT (135 Ci/mmol) were from NEN (Perkin-Elmer). Competitive inhibition assays were performed according to standard procedures, briefly detailed below.

**5-HT<sub>7</sub> Receptor.** Cell paste (6.8 mg/mL) was homogenized in 200 volumes of assay buffer (50 mM Tris-HCl, 10 mM MgSO<sub>4</sub>, 0.5 mM EDTA, pH 7.4 at 25 °C). Fractions of 500 μL of the membranes suspension were incubated at 27 °C for 120 min with 3 nM [<sup>3</sup>H]LSD, in the presence or absence of the competing drug, in a final volume of 540 μL of assay buffer. Nonspecific binding was determined by radioligand binding in the presence of a saturating concentration of 25 μM clozapine, and represented less than 15% of total binding.

**5-HT<sub>1A</sub> Receptor.** Cell paste (36.8 mg/mL) was homogenized in 29.1 volumes of assay buffer (50 mM Tris-HCl, 5 mM MgSO<sub>4</sub>, pH 7.4 at 25 °C). Fractions of 20 μL of the membranes suspension were incubated in the dark at 37 °C for 120 min with 4.9 nM [<sup>3</sup>H]-8-OH-DPAT, in the presence or absence of the competing drug, in a final volume of 200 μL of assay buffer. Nonspecific binding was determined by radioligand binding in the presence of a saturating concentration of 10 μM 5-HT, and represented less than 20% of total binding.

For all binding assays, competing drug, nonspecific, total, and radioligand bindings were defined in triplicate. Incubation was terminated by rapid vacuum filtration through Wallac Filtermat A filters, presoaked in poly(ethylenimine) (0.3% for the 5-HT<sub>7</sub>R and 0.5% for the 5-HT<sub>1A</sub>R), using a FilterMate Unifilter 96-Harvester. The filters were then washed 9 times with 500 μL of ice-cold 50 mM Tris-HCl buffer (pH 7.4 at 25 °C), and heated at 80 °C. The radioactivity bound to the filters was measured by scintillation spectrometry, using a Microbeta TopCount instrument. The data were analyzed by an iterative curve-fitting procedure (program Prism, Graph Pad), which provided IC<sub>50</sub>, K<sub>i</sub>, and r<sup>2</sup> values for test compounds, K<sub>i</sub> values being calculated from the Cheng–Prusoff equation.<sup>32</sup>

**5-HT<sub>7</sub>R Adenylate Cyclase Assay.** Effects on adenylate cyclase activity were determined at CEREP (Le Bois l'Eveque, 86600 Celle L'Evescault, France) according to previously published methods.<sup>39</sup> Briefly, CHO cells expressing the h5-HT<sub>7</sub>R were incubated at 37

°C for 45 min with the ligand, in the absence or presence of 100 nM serotonin, and the cAMP concentration was measured by HTRF. Adenylate cyclase activity is expressed as the percentage of the maximal effect obtained with 10  $\mu$ M serotonin. EC<sub>50</sub> and IC<sub>50</sub> values were calculated by nonlinear regression analysis of the concentration–response curves using Hill software developed at CEREP.

**Computational Methods. Models of the Ligand–Receptor Complexes.** Models of the TM domains 1–7 of the 5-HT<sub>7</sub> and 5-HT<sub>1A</sub> receptors were constructed by homology modeling techniques using the crystal structure of the  $\beta_2$ -adrenergic receptor (PDB code 2RH1)<sup>35,36</sup> as template. SCWRL-3.0<sup>44</sup> was employed to add the side chains of the nonconserved residues, using a backbone-dependent rotamer library. Modeler 9v1<sup>45</sup> was used to add intracellular loops IL1–2 and extracellular loops EL1–3 using the structure of the  $\beta_2$ -adrenergic receptor as template. Internal water molecules 506, 519, 528, 529, 532, 534, 537, 543, 546, and 548, that mediate a number of interhelical interactions<sup>36</sup> and seem conserved in the rhodopsin-like family of GPCRs,<sup>46</sup> were also included in the model. The Duan et al. (2003) force field<sup>47</sup> was used for peptides, and the general Amber force field (GAFF)<sup>48</sup> and HF/6-31G\*-derived RESP atomic charges were used for the ligands. Molecular dynamics simulations of the ligand–receptor complexes were performed with the Sander module of AMBER 9<sup>49</sup> using the protocol previously described.<sup>41</sup>

**Acknowledgment.** This work has been supported by grants from the Spanish Ministerio de Educación (MEC, SAF-2007/67008), Comunidad Autónoma de Madrid (CAM, S-SAL-249-2006), Instituto de Salud Carlos III (RD07/0067/0008), and AGAUR (SGR2005-00390). The authors thank MEC for predoctoral grants to R.A.M. and J.S.

**Supporting Information Available:** Synthesis of compound 22, spectral characterization data of compounds 22, 26, 27, 29, 1, 4, 5, 7–9, 11–15, and combustion analysis data. This material is available free of charge via the Internet at <http://pubs.acs.org>.

## References

- Nichols, D. E.; Nichols, C. D. Serotonin receptors. *Chem. Rev.* **2008**, *108*, 1614–1641.
- Hoyer, D.; Hannon, J. P.; Martin, G. R. Molecular, pharmacological and functional diversity of 5-HT receptors. *Pharmacol. Biochem. Behav.* **2002**, *71*, 533–554.
- Lydiard, R. B. An overview of generalized anxiety disorder: disease state-appropriate therapy. *Clin. Ther.* **2000**, *22* (Suppl. A), A3–19.
- Visser, W. H.; de Vriend, R. H.; Jaspers, M. W.; Ferrari, M. D. Sumatriptan in clinical practice: a 2-year review of 453 migraine patients. *Neurology* **1996**, *47*, 46–51.
- Milne, R. J.; Heel, R. C. Ondansetron. Therapeutic use as an antiemetic. *Drugs* **1991**, *41*, 574–595.
- Hedlund, P. B.; Sutcliffe, J. G. Functional, molecular and pharmacological advances in 5-HT<sub>7</sub> receptor research. *Trends Pharmacol. Sci.* **2004**, *25*, 481–486.
- Thomas, D. R.; Hagan, J. J. 5-HT<sub>7</sub> receptors. *Curr. Drug Targets CNS Neurol. Disord.* **2004**, *3*, 81–90.
- Plassat, J. L.; Amlaiky, N.; Hen, R. Molecular cloning of a mammalian serotonin receptor that activates adenylate cyclase. *Mol. Pharmacol.* **1993**, *44*, 229–236.
- Ruat, M.; Traiffort, E.; Leurs, R.; Tardivel-Lacombe, J.; Diaz, J.; Arrang, J. M.; Schwartz, J. C. Molecular cloning, characterization, and localization of a high-affinity serotonin receptor (5-HT<sub>7</sub>) activating cAMP formation. *Proc. Natl. Acad. Sci. U.S.A.* **1993**, *90*, 8547–8551.
- Lovenberg, T. W.; Baron, B. M.; de Lecea, L.; Miller, J. D.; Prosser, R. A.; Rea, M. A.; Foye, P. E.; Racke, M.; Slone, A. L.; Siegel, B. W.; Danielson, P. E.; Sutcliffe, J. G.; Erlander, M. G. A novel adenylyl cyclase-activating serotonin receptor (5-HT<sub>7</sub>) implicated in the regulation of mammalian circadian rhythms. *Neuron* **1993**, *11*, 449–458.
- Thomas, D. R.; Atkinson, P. J.; Hastie, P. G.; Roberts, J. C.; Middlemiss, D. N.; Price, G. W. [<sup>3</sup>H]-SB-269970 radiolabels 5-HT<sub>7</sub> receptors in rodent, pig and primate brain tissues. *Neuropharmacology* **2002**, *42*, 74–81.
- Sprouse, J.; Li, X.; Stock, J.; McNeish, J.; Reynolds, L. Circadian rhythm phenotype of 5-HT<sub>7</sub> receptor knockout mice: 5-HT and 8-OH-DPAT-induced phase advances of SCN neuronal firing. *J. Biol. Rhythms* **2005**, *20*, 122–131.
- Hedlund, P. B.; Huitron-Resendiz, S.; Henriksen, S. J.; Sutcliffe, J. G. 5-HT<sub>7</sub> receptor inhibition and inactivation induce antidepressant-like behavior and sleep pattern. *Biol. Psychiatry* **2005**, *58*, 831–837.
- Roberts, A. J.; Krucker, T.; Levy, C. L.; Slanina, K. A.; Sutcliffe, J. G.; Hedlund, P. B. Mice lacking 5-HT receptors show specific impairments in contextual learning. *Eur. J. Neurosci.* **2004**, *19*, 1913–1922.
- Terron, J. A.; Falcon-Neri, A. Pharmacological evidence for the 5-HT<sub>7</sub> receptor mediating smooth muscle relaxation in canine cerebral arteries. *Br. J. Pharmacol.* **1999**, *127*, 609–616.
- Prins, N. H.; Briejer, M. R.; Van Bergen, P. J.; Akkermans, L. M.; Schuurkes, J. A. Evidence for 5-HT<sub>7</sub> receptors mediating relaxation of human colonic circular smooth muscle. *Br. J. Pharmacol.* **1999**, *128*, 849–852.
- Terron, J. A. Is the 5-HT(7) receptor involved in the pathogenesis and prophylactic treatment of migraine? *Eur. J. Pharmacol.* **2002**, *439*, 1–11.
- De Ponti, F.; Tonini, M. Irritable bowel syndrome: new agents targeting serotonin receptor subtypes. *Drugs* **2001**, *61*, 317–332.
- Lovell, P. J.; Bromidge, S. M.; Dabbs, S.; Duckworth, D. M.; Forbes, I. T.; Jennings, A. J.; King, F. D.; Middlemiss, D. N.; Rahman, S. K.; Saunders, D. V.; Collin, L. L.; Hagan, J. J.; Riley, G. J.; Thomas, D. R. A novel, potent, and selective 5-HT(7) antagonist: (R)-3-(2-(4-methylpiperidin-1-yl)ethyl)pyrrolidine-1-sulfonyl phenol (SB-269970). *J. Med. Chem.* **2000**, *43*, 342–345.
- Forbes, I. T.; Cooper, D. G.; Dodds, E. K.; Douglas, S. E.; Gribble, A. D.; Ife, R. J.; Lightfoot, A. P.; Meeson, M.; Campbell, L. P.; Coleman, T.; Riley, G. J.; Thomas, D. R. Identification of a novel series of selective 5-HT<sub>7</sub> receptor antagonists. *Bioorg. Med. Chem. Lett.* **2003**, *13*, 1055–1058.
- Kikuchi, C.; Suzuki, H.; Hiranuma, T.; Koyama, M. New tetrahydrobenzindoles as potent and selective 5-HT(7) antagonists with increased in vitro metabolic stability. *Bioorg. Med. Chem. Lett.* **2003**, *13*, 61–64.
- Leopoldo, M.; Berardi, F.; Colabufo, N. A.; Contino, M.; Lacivita, E.; Niso, M.; Perrone, R.; Tortorella, V. Structure-affinity relationship study on N-(1,2,3,4-tetrahydronaphthalen-1-yl)-4-aryl-1-piperazinealkylamides, a new class of 5-hydroxytryptamine<sub>7</sub> receptor agents. *J. Med. Chem.* **2004**, *47*, 6616–6624.
- López-Rodríguez, M. L.; Porras, E.; Benhamú, B.; Ramos, J. A.; Morcillo, M. J.; Lavandera, J. L. First pharmacophoric hypothesis for 5-HT<sub>7</sub> antagonism. *Bioorg. Med. Chem. Lett.* **2000**, *10*, 1097–1100.
- López-Rodríguez, M. L.; Porras, E.; Morcillo, M. J.; Benhamú, B.; Soto, L. J.; Lavandera, J. L.; Ramos, J. A.; Olivella, M.; Campillo, M.; Pardo, L. Optimization of the pharmacophore model for 5-HT<sub>7</sub>R antagonism. Design and synthesis of new naphtholactam and naphthosultam derivatives. *J. Med. Chem.* **2003**, *46*, 5638–5650.
- Vermeulen, E. S.; Schmidt, A. W.; Sprouse, J. S.; Wikstrom, H. V.; Grol, C. J. Characterization of the 5-HT(7) receptor. Determination of the pharmacophore for 5-HT(7) receptor agonism and CoMFA-based modeling of the agonist binding site. *J. Med. Chem.* **2003**, *46*, 5365–5374.
- Vermeulen, E. S.; van Smeden, M.; Schmidt, A. W.; Sprouse, J. S.; Wikstrom, H. V.; Grol, C. J. Novel 5-HT<sub>7</sub> receptor inverse agonists. Synthesis and molecular modeling of arylpiperazine- and 1,2,3,4-tetrahydroisoquinoline-based arylsulfonamides. *J. Med. Chem.* **2004**, *47*, 5451–5466.
- Kolaczkowski, M.; Nowak, M.; Pawlowski, M.; Bojarski, A. J. Receptor-based pharmacophores for serotonin 5-HT<sub>7</sub>R antagonists-implications to selectivity. *J. Med. Chem.* **2006**, *49*, 6732–6741.
- Norman, M. H.; Rigdon, G. C.; Navas, F. III.; Cooper, B. R. Cyclic benzamides as mixed dopamine D<sub>2</sub>/serotonin 5-HT<sub>2</sub> receptor antagonists: potential atypical antipsychotic agents. *J. Med. Chem.* **1994**, *37*, 2552–2563.
- Nishiyama, M.; Yamamoto, T.; Koie, Y. Synthesis of N-arylpiperazines from aryl halides and piperazine under a palladium tri-tert-butylphosphine catalyst. *Tetrahedron Lett.* **1998**, *39*, 617–620.
- López-Rodríguez, M. L.; Benhamú, B.; Ayala, D.; Rominguer, J. L.; Murcia, M.; Ramos, J. A.; Viso, A. Pd(0) amination of benzimidazoles as an efficient method towards new (benzimidazolyl)piperazines with high affinity for the 5-HT(1A) receptor. *Tetrahedron* **2000**, *56*, 3245–3253.
- Gauthier, S.; Cloutier, J.; Dory, Y. L.; Favre, A.; Mailhot, J.; Ouellet, C.; Schwerdtfeger, A.; Merand, Y.; Martel, C.; Simard, J.; Labrie, F. Synthesis and structure-activity relationships of analogs of EM-652 (acolfibene), a pure selective estrogen receptor modulator. Study of nitrogen substitution. *J. Enzyme Inhib. Med. Chem.* **2005**, *20*, 165–177.
- Cheng, Y.; Prusoff, W. H. Relationship between the inhibition constant (K<sub>i</sub>) and the concentration of inhibitor which causes 50% inhibition (I<sub>50</sub>) of an enzymatic reaction. *Biochem. Pharmacol.* **1973**, *22*, 3099–3108.

- (33) Shi, L.; Javitch, J. A. The binding site of aminergic G protein-coupled receptors: the transmembrane segments and second extracellular loop. *Annu. Rev. Pharmacol. Toxicol.* **2002**, *42*, 437–467.
- (34) Warne, T.; Serrano-Vega, M. J.; Baker, J. G.; Moukhametzianov, R.; Edwards, P. C.; Henderson, R.; Leslie, A. G.; Tate, C. G.; Schertler, G. F. Structure of a beta1-adrenergic G-protein-coupled receptor. *Nature* **2008**, *454*, 486–91.
- (35) Cherezov, V.; Rosenbaum, D. M.; Hanson, M. A.; Rasmussen, S. G.; Thian, F. S.; Kobilka, T. S.; Choi, H. J.; Kuhn, P.; Weis, W. I.; Kobilka, B. K.; Stevens, R. C. High-resolution crystal structure of an engineered human beta2-adrenergic G protein-coupled receptor. *Science* **2007**, *318*, 1258–1265.
- (36) Rosenbaum, D. M.; Cherezov, V.; Hanson, M. A.; Rasmussen, S. G.; Thian, F. S.; Kobilka, T. S.; Choi, H. J.; Yao, X. J.; Weis, W. I.; Stevens, R. C.; Kobilka, B. K. GPCR engineering yields high-resolution structural insights into beta2-adrenergic receptor function. *Science* **2007**, *318*, 1266–1273.
- (37) Smit, M. J.; Vischer, H. F.; Bakker, R. A.; Jongejan, A.; Timmerman, H.; Pardo, L.; Leurs, R. Pharmacogenomic and structural analysis of constitutive G protein-coupled receptor activity. *Annu. Rev. Pharmacol. Toxicol.* **2007**, *47*, 53–87.
- (38) Bojarski, A. J.; Duszynska, B.; Kolaczowski, M.; Kowalski, P.; Kowalska, T. The impact of spacer structure on 5-HT<sub>7</sub> and 5-HT<sub>1A</sub> receptor affinity in the group of long-chain arylpiperazine ligands. *Bioorg. Med. Chem. Lett.* **2004**, *14*, 5863–5866.
- (39) Adham, N.; Zgombick, J. M.; Bard, J.; Branchek, T. A. Functional characterization of the recombinant human 5-hydroxytryptamine<sub>7(a)</sub> receptor isoform coupled to adenylate cyclase stimulation. *J. Pharmacol. Exp. Ther.* **1998**, *287*, 508–514.
- (40) Schwartz, T. W.; Frimurer, T. M.; Holst, B.; Rosenkilde, M. M.; Elling, C. E. Molecular mechanism of 7TM receptor activation—a global toggle switch model. *Annu. Rev. Pharmacol. Toxicol.* **2006**, *46*, 481–519.
- (41) Jongejan, A.; Bruysters, M.; Ballesteros, J. A.; Haaksma, E.; Bakker, R. A.; Pardo, L.; Leurs, R. Linking agonist binding to histamine H<sub>1</sub> receptor activation. *Nat. Chem. Biol.* **2005**, *1*, 98–103.
- (42) López-Rodríguez, M. L.; Morcillo, M. J.; Fernández, E.; Benhamú, B.; Tejada, I.; Ayala, D.; Viso, A.; Campillo, M.; Pardo, L.; Delgado, M.; Manzanares, J.; Fuentes, J. A. Synthesis and structure-activity relationships of a new model of arylpiperazines. 8. Computational simulation of ligand-receptor interaction of 5-HT(1A)R agonists with selectivity over alpha1-adrenoceptors. *J. Med. Chem.* **2005**, *48*, 2548–58.
- (43) Boar, B. R.; O'Shea, D. M.; Tomlinson, I. D. 1-Substituted isatin and oxindole derivatives as inhibitors of acetylcholinesterase. PCT Int. Appl. WO 94/29272, 1994.
- (44) Canutescu, A. A.; Shelenkov, A. A.; Dunbrack, R. L. Jr. A graph-theory algorithm for rapid protein side-chain prediction. *Protein Sci.* **2003**, *12*, 2001–2014.
- (45) Marti-Renom, M. A.; Stuart, A. C.; Fiser, A.; Sanchez, R.; Melo, F.; Sali, A. Comparative protein structure modeling of genes and genomes. *Annu. Rev. Biophys. Biomol. Struct.* **2000**, *29*, 291–325.
- (46) Pardo, L.; Deupí, X.; Dolker, N.; López-Rodríguez, M. L.; Campillo, M. The role of internal water molecules in the structure and function of the rhodopsin family of G protein-coupled receptors. *ChemBioChem* **2007**, *8*, 19–24.
- (47) Duan, Y.; Wu, C.; Chowdhury, S.; Lee, M. C.; Xiong, G.; Zhang, W.; Yang, R.; Cieplak, P.; Luo, R.; Lee, T.; Caldwell, J.; Wang, J.; Kollman, P. A point-charge force field for molecular mechanics simulations of proteins based on condensed-phase quantum mechanical calculations. *J. Comput. Chem.* **2003**, *24*, 1999–2012.
- (48) Wang, J.; Wolf, R. M.; Caldwell, J. W.; Kollman, P. A.; Case, D. A. Development and testing of a general amber force field. *J. Comput. Chem.* **2004**, *25*, 1157–1174.
- (49) Case, D. A.; Darden, T. A.; Cheatham, T. E. I.; Simmerling, C. L.; Wang, J.; Duke, R. E.; Luo, R.; Merz, K. M.; Pearlman, D. A.; Crowley, M.; Walker, R. C.; Zhang, W.; Wang, B.; Hayik, S.; Roitberg, A.; Seabra, G.; Wong, K. F.; Paesani, F.; Wu, X.; Brozell, S.; Tsui, V.; Gohlke, H.; Yang, L.; Tan, C.; Mongan, J.; Hornak, V.; Cui, G.; Beroza, P.; Matthews, D. H.; Schafmeister, C.; Ross, W. S.; Kollman, P. A. *AMBER 9*; University of California: San Francisco, 2006.

JM8014553